Manipulating PML SUMOylation via Silencing UBC9 and RNF4 Regulates Cardiac Fibrosis

Yu Liu,[1,3] Dan Zhao,[2,3] Fang Qiu,[1,3] Ling-Ling Zhang,[1] Shang-Kun Liu,[1] Yuan-Yuan Li,[1] Mei-Tong Liu,[1] Di Wu,[1] Jia-Xin Wang,[1] Xiao-Qing Ding,[2] Yan-Xin Liu,[1] Chang-Jiang Dong,[1] Xiao-Qi Shao,[1] Bao-Feng Yang,[1] and Wen-Feng Chu[1]

[1]Department of Pharmacology, The State-Province Key Laboratories of Biomedicine Pharmaceutics of China, Key Laboratory of Cardiovascular Research, Ministry of Education, College of Pharmacy, Harbin Medical University at Harbin, Heilongjiang 150081, P.R. China; [2]Department of Clinical Pharmacy, Key Laboratories of Education Ministry for Myocardial Ischemia Mechanism and Treatment, The 2nd Affiliated Hospital, Harbin Medical University at Harbin, Heilongjiang 150081, P.R. China

The promyelocytic leukemia protein (PML) is essential in the assembly of dynamic subnuclear structures called PML nuclear bodies (PML-NBs), which are involved in regulating diverse cellular functions. However, the possibility of PML being involved in cardiac disease has not been examined. In mice undergoing transverse aortic constriction (TAC) and arsenic trioxide (ATO) injection, transforming growth factor β1 (TGF-β1) was upregulated along with dynamic alteration of PML SUMOylation. In cultured neonatal mouse cardiac fibroblasts (NMCFs), ATO, angiotensin II (Ang II), and fetal bovine serum (FBS) significantly triggered PML SUMOylation and the assembly of PML-NBs. Inhibition of SUMOylated PML by silencing UBC9, the unique SUMO E2-conjugating enzyme, reduced the development of cardiac fibrosis and partially improved cardiac function in TAC mice. In contrast, enhancing SUMOylated PML accumulation, by silencing RNF4, a poly-SUMO-specific E3 ubiquitin ligase, accelerated the induction of cardiac fibrosis and promoted cardiac function injury. PML colocalized with Pin1 (a positive regulator for TGF-β1 mRNA expression in PML-NBs) and increased TGF-β1 activity. These findings suggest that the UBC9/PML/RNF4 axis plays a critical role as an important SUMO pathway in cardiac fibrosis. Modulating the protein levels of the pathway provides an attractive therapeutic target for the treatment of cardiac fibrosis and heart failure.

INTRODUCTION

Heart failure is a major risk factor in human health and a prevalent cause of both morbidity and mortality.[1] Cardiac fibrosis is a common morphological feature that is characterized by structural remodeling of the cardiac interstitium, which can lead to increased stiffness and diastolic dysfunction.[2] The pleiotropic cytokine transforming growth factor β1 (TGF-β1) plays a critical role in cardiac fibrosis as a key mediator in cardiac ventricular remodeling. This remodeling results in the abnormal accumulation of fibrillar collagen, which contributes to excessive extracellular matrix deposition and affects overall function of fibroblasts through both the canonical Smad and non-canonical signaling.[3,4] Despite the fact that extensive studies have been published, the underlying mechanisms for TGF-β1 expression regulation remain poorly understood.

The promyelocytic leukemia protein (PML) gene was originally discovered through its fusion with the RAR gene, which can cause acute promyelocytic leukemia. SUMOylation, a post-translational modification, is accomplished by the covalent binding of the small ubiquitin-like modifier (SUMO) to a target protein lysine residue, which is regulated by UBC9, a unique SUMO E2-conjugating enzyme responsible for substrate recognition.[5] Notably, Zhang et al. revealed that acute promyelocytic leukemia is highly sensitive to arsenic trioxide (ATO) chemotherapy. ATO can bind directly to the PML protein, resulting in covalent modification of PML by SUMOs; namely, PML SUMOylation[6] and PML degradation via RNF4, an E3 ubiquitin ligase family member, through the ubiquitin-mediated pathway.[7] PML is a key organizer of nuclear bodies (NBs) that recruit a number of regulatory proteins that are implicated in the regulation of many biological processes such as senescence, viral infection, and DNA damage.[8] However, the function of PML in the heart remains to be elucidated. Our group has previously demonstrated that ATO can cause significant cardiac fibrosis by increasing TGF-β1 expression.[9] These facts promoted us to propose that the PML-associated SUMO processes may be a critical regulator of cardiac fibrosis.

Herein, we identified UBC9/PML/RNF4 as novel mediators of the SUMO pathway of cardiac fibrosis and unraveled that modulating these protein levels regulates TGF-β1 expression through the sequestering of a peptidyl-prolyl isomerase, Pin1, by PML-NBs.
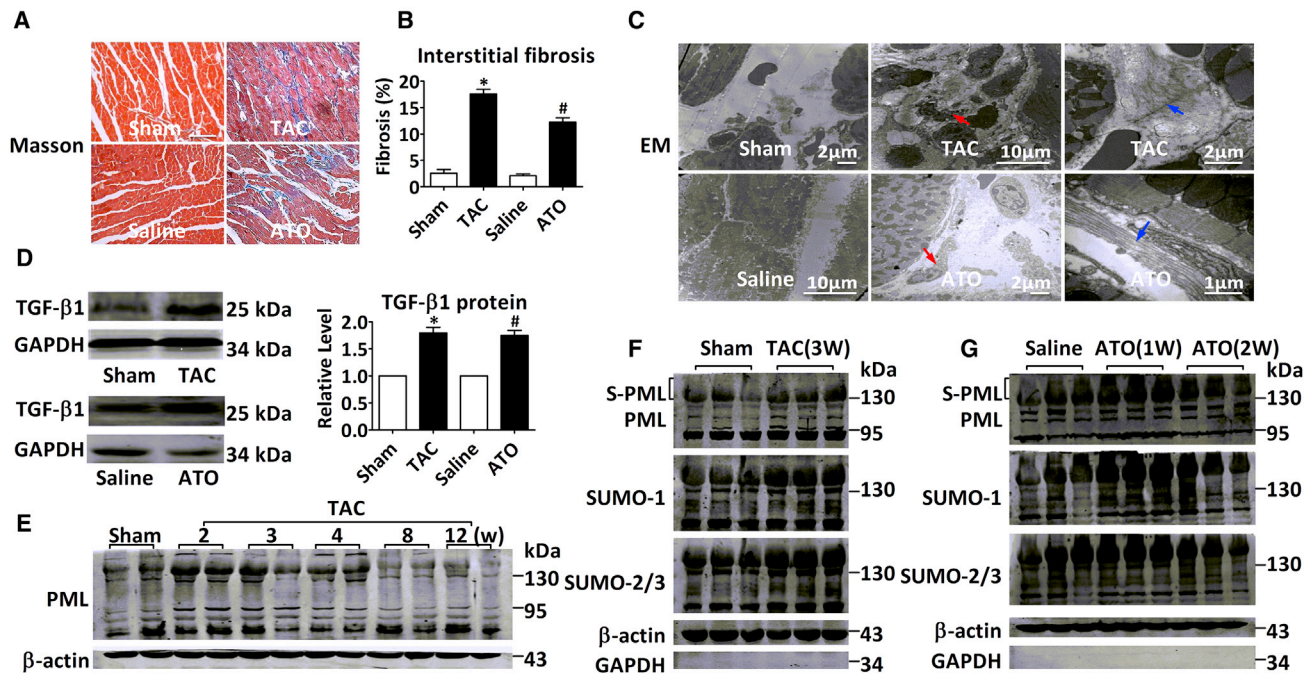
Figure 1. Alterations of PML SUMOylation in Mouse Models of Cardiac Fibrosis

(A and B) Masson's trichrome-stained images in histological sections with the area of fibrosis (blue) in the left ventricle quantified after TAC for 3 weeks and ATO injection (2 mg/kg) for 1 week. Scale bar, 100 μm. (C) Representative electron microscopy (EM) images showing the characteristic changes and collagen production in the left ventricle of the fibrotic mice. The red arrow indicates cardiac fibroblasts, and the blue arrow indicates collagen. (D) Representative immunoblots and quantitative results of TGF-β1 expression in the left ventricle. GAPDH served as a loading control. (E) Immunoblotting analysis of PML in mouse hearts at 2, 3, 4, 8, and 12 weeks post-TAC surgery, with β-actin used as a loading control. (F and G) Immunoblotting analysis of PML in nuclear extracts from models established by (F) TAC for 3 weeks (3W) or (G) injected with ATO for 1 or 2 weeks (1W and 2W, respectively). GAPDH and β-actin were used as internal controls for cytoplasmic and nuclear fractions, respectively. The molecular weight in kilodaltons is shown on the right side of the each blot. S-PML, SUMOylated PML. n = 6 per group in (A)–(F) from three independent experiments with similar results. Data are normalized to GAPDH and expressed as mean ± SEM, *p < 0.05 versus sham; #p < 0.05 versus saline.

RESULTS

Alteration of SUMOylated PML in the Experimental Cardiac Fibrotic Models Induced by Pressure Overload and by ATO

In order to gain insights into the possible role of PML SUMOylation in cardiac fibrosis, we used two different experimental fibrotic models: the TAC (transverse aortic constriction)-induced pressure overload model and the ATO-injection (2 mg/kg) model. Masson staining analysis demonstrated significant interstitial collagen deposition in the left ventricular (LV) myocardium in both TAC mice (3 weeks) and ATO-injected mice (1 week) (Figures 1A and 1B). Meanwhile, electron microscopic examination revealed considerable proliferation of cardiac fibroblasts and aberrant accumulation of collagen fibers in both models compared with control mice (Figure 1C). Furthermore, immunoblotting analysis indicated that TGF-β1 expression was elevated in the ventricular myocardium of both fibrotic models (Figure 1D).

In order to understand the role of PML in the development of cardiac fibrosis, PML protein expression was examined in mice at different time points post-TAC surgery. In the TAC models, the high-molecular-weight (HMW) PML species (>130 kDa) were increased initially within 2 and 3 weeks post-TAC operation and subsequently declined sharply by 8 weeks post-surgery (Figure 1E). After SUMO modification, PML migrated from the nucleoplasm toward the subnuclear structure NBs.[10] Thus, unmodified PML was found in the soluble fraction of the nucleus, while the SUMO-modified forms appeared as HMW species.[11] We then furthered our study to understand the dynamic process of PML SUMOylation during pathological stress with the nuclear proteins extracted from heart tissues. Immunoblotting analysis revealed that PML isoforms with molecular weights >95 kDa were primarily located within the nucleus (Figure S1). Significant accumulation of the HMW PML isoforms with SUMO-1 and SUMO-2/3 conjugations was consistently observed in TAC mice (3 weeks) (Figure 1F). Similarly, the HMW PML isoforms and the SUMO molecules were increased 1 week after ATO-injected mice but subsequently declined by 2 weeks (Figure 1G). These results suggest that PML SUMOylation is dynamically regulated during the transition from the compensatory process to cardiac fibrosis and the associated structural remodeling.

PML SUMOylation Induced by ATO, Angiotensin II, and Fetal Bovine Serum in Cultured Neonatal Mouse Cardiac Fibroblasts

Next, the possible roles of PML SUMOylation in cardiac fibrosis were investigated in vitro. Neonatal mouse cardiac fibroblasts (NMCFs)
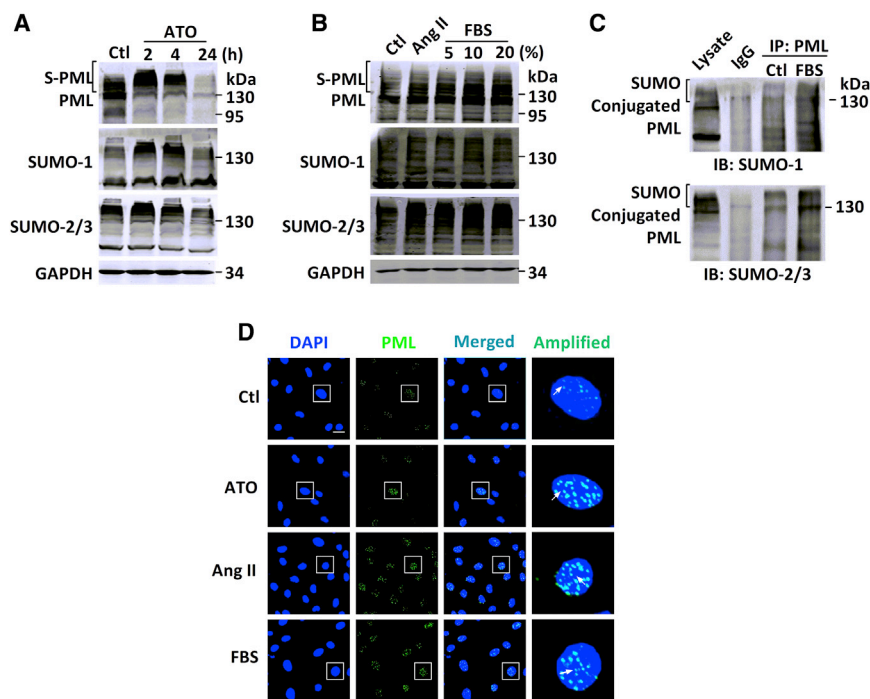
Figure 2. PML SUMOylation and NB Formation in a Cellular Model of Fibrosis with NMCFs

(A) Representative immunoblotting analysis examining the endogenous expression of PML (top), SUMO-1 (middle), and SUMO-2/3 (bottom) from whole-cell extracts of NMCFs after the addition of ATO for 2, 4, and 24 hr. Ctl, control. (B) Ang II or FBS at concentrations of 5%, 10%, and 20%. GAPDH was used as an internal control. The molecular weight in kilodaltons is shown on the right of each blot. S-PML, SUMOylated PML. The experiments shown are representative of three independent experiments with similar results. (C) Detection of PML conjugated with SUMO-1 (upper panel) or SUMO-2/3 (lower panel) in NMCFs was performed by co-IP after 20% FBS treatment. IgG, immunoglobulin G; IB, immunoblot. (D) Immunofluorescent analysis of NMCFs in response to ATO (2 μM) for 4-hr and 12-hr exposure to Ang II (100 nM) or FBS (20%), with PML (green) and the nuclei (blue), visualized with a laser confocal microscope. Scale bar, 25 μm. The boxed area in the merged picture is amplified for visualizing PML-NBs. White arrows indicate the PML-NBs. (A)–(C) are representative of three independent experiments with similar results.

were treated with 2 μM ATO, 100 nM angiotensin II (Ang II), and varying concentrations of fetal bovine serum (FBS) separately to establish in vitro fibrotic models. Immunoblotting analysis indicated that exposure to ATO for 2 or 4 hr triggered a dramatic shift toward PML SUMOylation, while prolonged exposure led to PML degradation as previously reported (Figure 2A).[12] As expected, exposure to either Ang II or FBS for 12 hr caused similar accumulation of the HMW PML isoforms. Interestingly, FBS also increased PML SUMOylation in a dose-dependent manner (Figure 2B). In immunoblotting analysis, the same bands were detected by SUMO-1 and SUMO-2/3 antibodies, suggesting differential expression of SUMOs in response to different fibrotic inducers. In order to detect SUMO-conjugated PML proteins, immunoprecipitation of proteins with PML antibodies under the denaturing conditions followed by immunoblotting with either SUMO-1 or SUMO-2/3 antibodies revealed multiple bands of HMWs (>130 kDa). These bands corresponded to the PML conjugated with SUMO molecules. In addition, FBS stimulation enhanced SUMO conjugation of PML in NMCFs (Figure 2C).

PML-NBs, the matrix-associated structures that are sensitive to varying stresses, can act as the platforms for recruitment of partners that regulate various biological events.[13] Consistent with the immunoblotting data on PML SUMOylation, immunohistochemical analysis showed that the size and number of PML-NBs in the nuclei were remarkably increased after the addition of ATO, Ang II, or FBS (Figure 2D). These results indicate that ATO, Ang II, and FBS are all able to trigger PML SUMOylation and PML-NB assembly in vitro.

Regulation of TGF-β1 Expression and Collagen Synthesis by PML SUMOylation via Silencing of UBC9 and RNF4

We then continued our investigations for in-depth understanding of the role of PML in cardiac fibrosis. To this end, a PML expression plasmid was transfected into NMCFs. Overexpression of PML promoted both the accumulation of unmodified (95 or 110 kDa) and SUMO-modified (>130 kDa) PML and activated TGF-β1 signaling and α-smooth muscle actin (α-SMA) protein expression (Figure 3A). Immunofluorescence analysis confirmed that PML overexpression promoted the expression of α-SMA and the differentiation of myofibroblasts in comparison with the empty-vector control group (Figure 3B). In contrast, knockdown of PML by its small interfering (si)RNAs effectively reduced the expression of both unmodified (95 or 110 kDa) and SUMO-modified (>30 kDa) PML (Figure 3C), as well as that of the pro-fibrotic factor-induced TGF-β1, p-Smad2/3, and α-SMA (Figures 3D–3F). These results indicated that PML protein caused differentiation of myofibroblasts through the TGF-β/*Smad* signaling pathway.

As SUMOylation is a key post-translational modification for maintaining the proper PML-NB structure and normal function, the role of PML SUMOylation in cardiac fibrosis was further evaluated using the siRNAs against UBC9 or RNF4. UBC9 serves as the single E2-conjugating enzyme and, therefore, is essential for SUMO conjugation to its substrates.[14] The efficiencies of UBC9 and RNF4 knockdown by their respective siRNAs were verified (Figures S2A and S2B). The co-immunoprecipitation (co-IP) results clearly indicated the specific role of the common
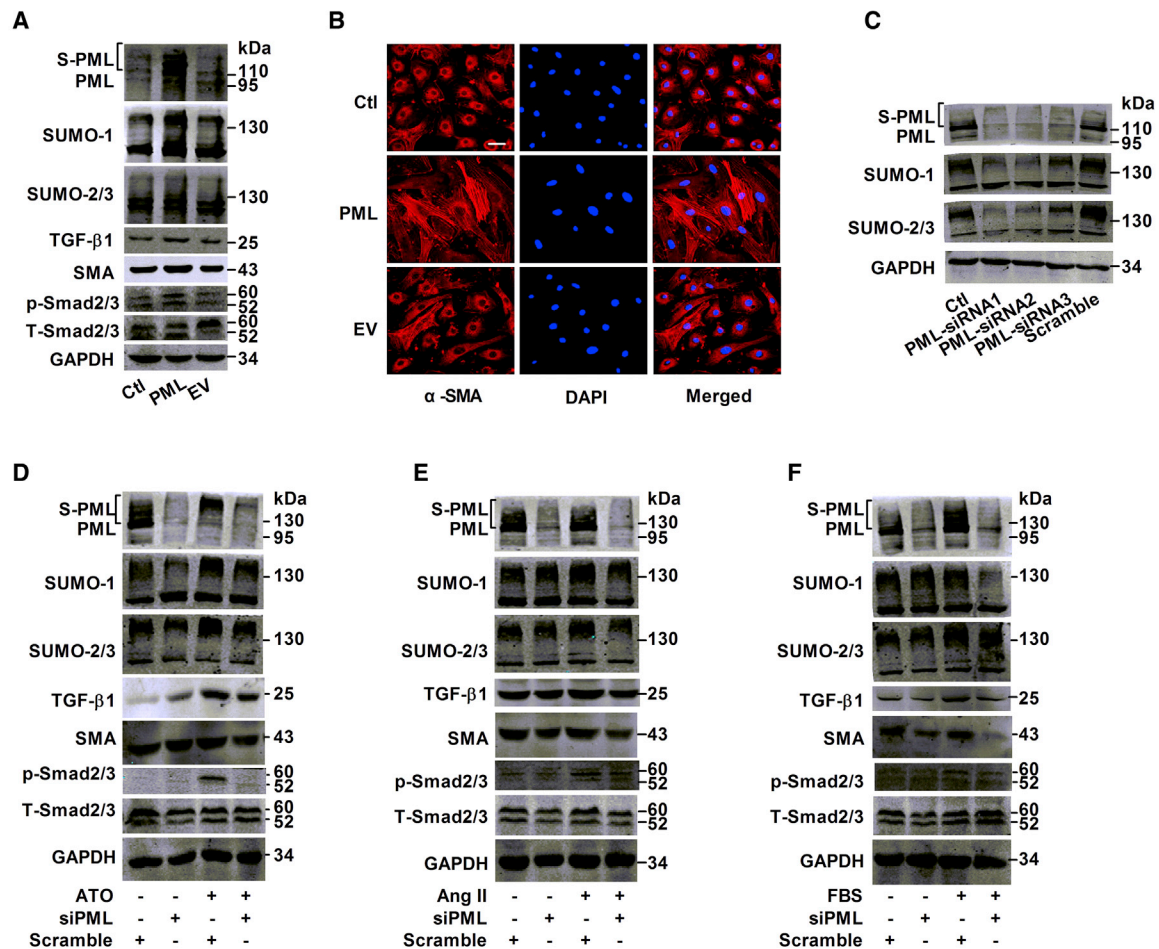
Figure 3. Overexpression or Knockdown of PML Activated the TGF-β1 Signaling and α-SMA Protein Expression in NMCFs

(A) The expression of PML, SUMO-1, SUMO-2/3, TGF-β1, α-SMA (SMA), and p-Smad2/3 in PML-overexpressing NMCFs by immunoblotting analysis. Ctl, control; EV, empty vector. (B) Representative images of α-SMA (red) and nuclei (blue) obtained from PML overexpression NMCFs. Scale bar, 25 μm. (C) PML, SUMO-1, and SUMO-2/3 expression in PML extinction NMCFs by siRNAs. (D–F) The expression of PML, SUMO-1, SUMO-2/3, TGF-β1, α-SMA, and p-Smad2/3 in PML-silenced NMCFs by immunoblotting analysis. The data shown in (A)–(F) are representative of three independent experiments with similar results.

E2-conjugating enzyme, UBC9, in PML SUMOylation, as reflected by the data showing that depletion of UBC9 reduced SUMO-1 and SUMO-2/3 conjugation of the HMW PML, compared with the FBS-treatment group (Figure S2C). Immunoblotting showed that treatment with 2 μM ATO for 4 hr and 100 nM Ang II or 20% FBS for 12 hr increased TGF-β1 protein (Figures 4A–4C) and mRNA (Figures 4G–4I) expression levels. However, a loss of UBC9 not only alleviated PML SUMOylation (Figures 4A–4C) induced by multiple pro-fibrotic factors but also suppressed the TGF-β1 signaling by decreasing the expression of TGF-β1 at both the mRNA (Figures 4G–4I) and protein (Figures 4A–4C) levels and the levels of p-Smad2/3, the activated form of Smad2/3 (Figures S3A–S3C and S3G), in comparison with the fibrotic-stimulation groups. Meanwhile, silencing UBC9 reduced collagen production (Figures 4J–4L) in response to ATO, Ang II, and FBS stimulation in NMCFs.

RNF4, the well-known ubiquitin E3 ligase, is responsible for PML degradation[15] and caused the accumulation of PML SUMOylation when silenced by its siRNA. Co-IP assays were performed to better assess the influence of RNF4 on PML-SUMO interactions. The increase in HMW SUMO conjugates indicated that RNF4 extinction further promoted SUMO-1 and SUMO-2/3 conjugation of PML, compared with the FBS-treatment group (Figure S2D). RNF4 knockdown by siRNA led to further accumulation of SUMOylated PML (Figures 4D–4F) and exacerbated ATO-, AngII-, and FBS-induced upregulation of TGF-β1 mRNA (Figures 4G–4I) and protein (Figures 4D–4F), as well as p-Smad2/3 levels (Figures S3D–S3F and S3H). As expected, RNF4 knockdown also promoted the excessive accumulation of the collagen content in NMCFs exposed to ATO, Ang II, and FBS (Figures 4J–4L). These results imply that intervention with UBC9 and RNF4 affects the PML SUMOylation process and exerts a strong effect on TGF-β1 expression and collagen production in NMCFs.
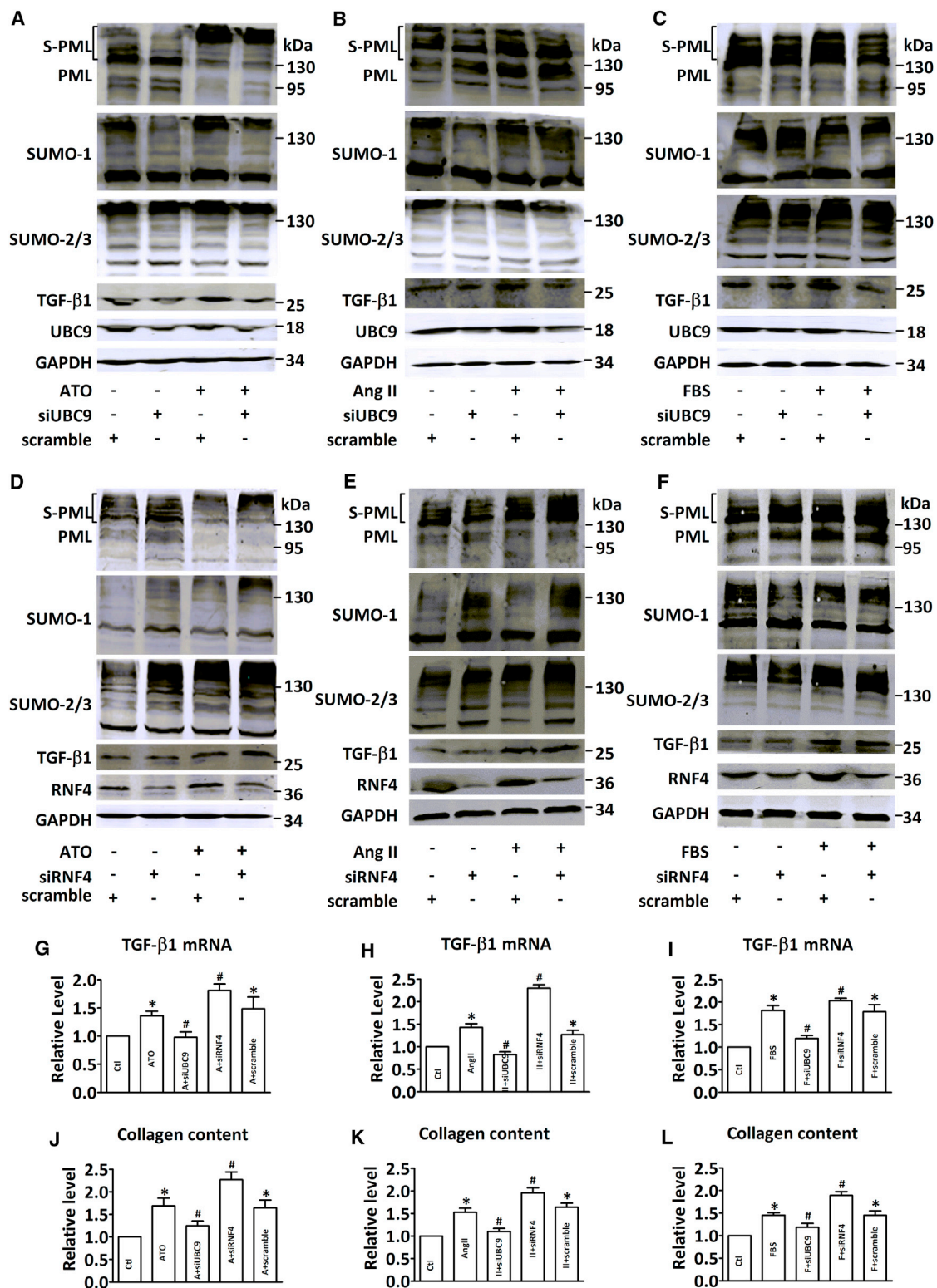
(legend on next page)

A similar mode of regulatory roles of UBC9/PML/RNF4 was observed in primary cultured cardiomyocytes with Ang II stimulation (Figure S4), in agreement with the results presented earlier for cardiac fibroblasts.

Regulation of Cardiac Fibrogenesis by PML SUMOylation through Cooperation between UBC9 and RNF4

In an effort to identify the involvement of the UBC9/PML/RNF4 axis in vivo, short hairpin RNA (shRNA) lentiviral vectors targeting UBC9 or RNF4 were delivered into mice through coronary arteries. After 7 days, mice were subjected to TAC operation, and the efficiencies of the silencing of UBC9 and RNF4 genes by their respective shRNAs were confirmed by immunofluorescence (Figure S5A). The mRNA levels of UBC9 and RNF4 in heart tissue, isolated cardiac fibroblasts, and cardiomyocytes were significantly decreased (Figures S5B and S5C). UBC9 and RNF4 protein levels were also correspondingly decreased, as revealed by immunoblotting analysis (Figures S5D and S5E).

Fibrosis is believed to be the key step of the structural remodeling for the transition from compensated hypertrophy to heart failure.[16] Masson staining demonstrated that lenti-shUBC9 promoted the regression of the severe fibrosis in TAC mice 3 weeks following the operation. Furthermore, electron-microscopic examination revealed the decreases in fibroblast proliferation and collagen deposition in the mice with knockdown of endogenous UBC9 (Figures 5A and 5B). Increase in the diffuse myocardial fibrosis is widely considered to be the leading cause of diastolic dysfunction.[17] TAC for 3 weeks exhibited an increased mitral E/A ratio (ratio of peak velocity of early to late filling of mitral inflow) and Tei index relative to the sham group, as demonstrated by Doppler echocardiography (Table 1). On the other hand, lenti-shUBC9 treatment improves diastolic function, as evidenced by a reduced mitral E/A ratio and Tei index (Table 1), compared to findings for the TAC mice. Likewise, echocardiography revealed the severe cardiac dysfunction during constant pressure overload for 12 weeks. Lenti-shUBC9 mice significantly improved the cardiac function, with elevated ejection fraction (EF) from 34.03% to 45.15% and fractional shortening (FS) from 16.24% to 22.73% (Figures 5C and 5D). These findings suggest that UBC9 knockdown could improve LV diastolic filling properties and systolic function by suppressing myocardial fibrosis.

Next, the association of PML SUMOylation and TGF-β1 expression with the cardiac function was assessed. Consistent with our in vitro results, UBC9 silencing alleviated the accumulation of the HMW PML (>130 kDa) and SUMO-1/2/3 conjugation caused by TAC (Figure 5E). Additionally, the typical fibrotic lesions caused by TAC appeared less frequently, and the expression of TGF-β1, a crucial pro-fibrotic cytokine,[4] at both the mRNA (Figure 5F) and protein levels (Figure 5G), was reduced, along with a reduction of Smad2/3 phosphorylation (Figures S6A and S6B). These findings suggested that inhibition of PML SUMOylation by lenti-shUBC9 mitigated cardiac remodeling and ameliorated cardiac dysfunction during the development of heart failure.

In contrast, compared to the TAC mice at 3 weeks, the lenti-shRNF4 injection significantly increased the extent of TAC-associated fibrosis, with abnormal accumulation of collagen in the hypertrophied myocardium (Figures 6A and 6B). Notably, RNF4 knockdown in the heart without TAC operation was able to directly induce collagen accumulation (Figure S5F). Similarly, the mice pretreated with lenti-RNF4 had more severe diastolic dysfunction, with a markedly decreased E/A ratio and Tei index, compared to TAC mice at 3 weeks (Table 1). Furthermore, the deterioration of cardiac function was found to be more pronounced in the lenti-shRNF4 mice at 8 weeks than in the TAC mice, with EF decreased from 57.01% to 39.01% and FS decreased from 29.36% to 18.97% (Figures 6C and 6D). Subsequently, PML SUMOylation (Figure 6E) and the expression of TGF-β1 (Figures 6F and 6G) and p-Smad2/3 (Figures S6A and S6B) were further aggravated after RNF4 knockdown. Collectively, PML SUMOylation was promoted following RNF4 knockdown, which, in turn, promoted the transition from cardiac hypertrophy to heart failure with impaired cardiac function.

The TAC-induced increase in the expression of cardiac β-myosin heavy chain (β-MHC) protein (Figure S6A), atrial natriuretic peptide (Figure S6C), and brain natriuretic peptide (Figure S6D) was significantly decreased by lentivirus-mediated knockdown of UBC9. In contrast, knockdown of RNF4 further aggravated the expression of these cardiac hypertrophic markers (Figures S6A–S6D). These findings correspond with our in vitro results that PML SUMOylation cooperation with UBC9 or RNF4 affected hypertrophic phenotypes, concomitant with remarkable changes in actin cytoskeleton structure and β-MHC protein expression in cultured cardiomyocytes (Figures S4A and S4B). Extensive evidence suggests that pressure overload triggers a transient inflammatory response in the myocardium. Our data showed that depletion of UBC9 decreased the mRNA levels of inflammatory cytokines, such as tumor necrosis factor α (TNF-α),

Figure 4. Silencing of UBC9 and RNF4 Regulates PML SUMOylation, TGF-β1 Expression, and Collagen Production in NMCFs
(A–F) In (A–C), representative immunoblotting analysis is shown of the endogenous expression of PML, SUMO-1, SUMO-2/3, and TGF-β1 in UBC9-silenced whole-cell extracts from NMCFs. (D–F) Representative immunoblotting analysis of the endogenous expression of PML, SUMO-1, SUMO-2/3, and TGF-β1 in whole-cell extracts from NMCFs after RNF4 knockdown. Data shown in (A)–(F) are representative of three independent experiments with similar results. (G–I) TGF-β1 mRNA levels were analyzed by real-time PCR in NMCFs after transfection with either siUBC9 or siRNF4 in response to ATO, Ang II, or FBS. (J–L) Statistical results for the collagen content was measured as described in NMCFs after transfection with either siUBC9 or siRNF4 for 6 hr in response to ATO, Ang II, or FBS for 24 hr. GAPDH was used as an internal control. Statistical differences in (G)–(L) were determined from five independent experiments. Data are represented as mean ± SEM. *p < 0.05 versus control; #p < 0.05 versus ATO, Ang II, or FBS.
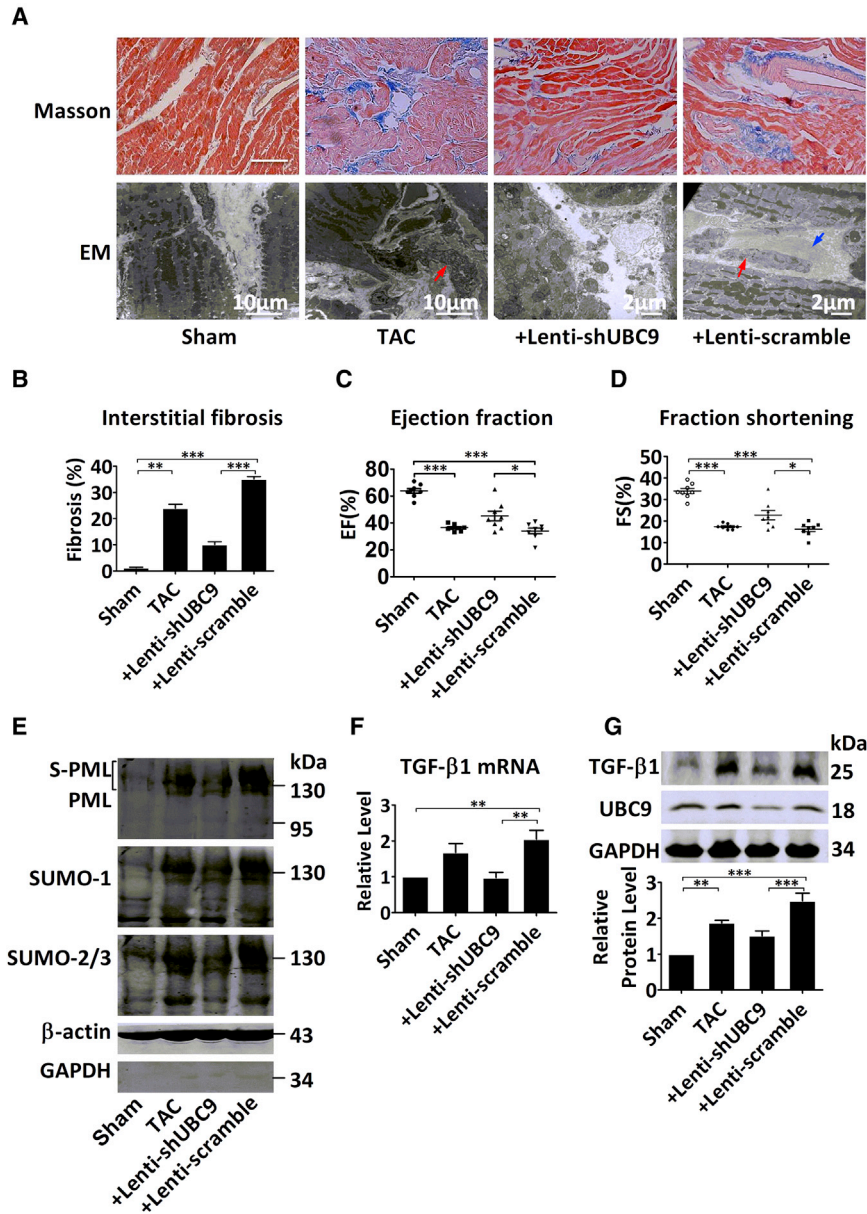
each other's partner protein. Notably, a specific PML isoform with a molecular mass of 95 kDa interacted with Pin1 and corresponded to the most extensively studied isoform (Figure 7A).[19,20]

Consistent with our co-IP results, PML and Pin1 were found co-localized under confocal microscopy in cultured NMCFs. Pin1 exhibited a diffuse distribution throughout the nucleus and a partial colocalization with PML (Figure 7B). Varying stimuli induced considerable aggregation of Pin1 onto PML-NBs and increased PML/Pin1 colocalization (Figure 7C). Moreover, immunofluorescence demonstrated a severe defect in NB assembly due to loss in NB number and intensity. Thus, the NBs were deficient in Pin1 recruitment and were mainly localized to the cytoplasm in response to the

interleukin (IL)-1β (IL-1β), IL-6, and IL-10 in comparison with the TAC group, while RNF4 ablation exacerbated the inflammatory response (Figures S7A–S7D).

Alterations of Sequestration of Pin1 to PML-NBs and Expression of TGF-β1 by Silencing UBC9 and RNF4

As already mentioned earlier, PML-NBs are matrix-associated structures that recruit an astonishing number of partner proteins, of which Pin1 deserves special attention, as it has been reported to stabilize TGF-β1 mRNA by mediating its association with ARE (AU-rich element)-binding proteins.[18] Our co-IP experiments confirmed that either anti-Pin1 or anti-PML antibodies were able to pull down

fibrotic stimuli in the absence of UBC9. Conversely, RNF4 knockdown yielded a dramatic increase in PML-NB number and size and enhanced the sequestration of Pin1 into the NBs (Figures 7C and S8). In the nuclear extracts from 3-week TAC model, the PML/Pin1 complex was increased relative to the sham mice, and lenti-shUBC9 reduced the formation of the PML/Pin1 complex (Figure 7D). Conversely, lenti-shRNF4 further enhanced the PML/Pin1 interactions (Figure 7E). In order to further investigate the role of Pin1 in TGF-β1 expression, Pin1 was selectively inhibited using Juglone,[21] which attenuated the increased expression of TGF-β1 (Figures 7F and 7G) in response to ATO, Ang II, and FBS. These results were further substantiated following knockdown of Pin1 by its siRNA

Table 1. Echocardiographic Analysis of Diastolic Function: Transmitral Doppler Parameters at 3 Weeks after TAC in Mice Pretreated with Lenti-shUBC9 or Lenti-shRNF4

Index	Sham (n = 10)	TAC (n = 10)	+Lenti-shUBC9 (n = 10)	+Lenti-shRNF4 (n = 10)	+Lenti-scramble (n = 11)
LV mass (mg)	1.28 ± 0.15	2.06 ± 0.25*	1.43 ± 0.11#	2.24 ± 0.25#	1.92 ± 0.22*
E (cm/s)	70.83 ± 10.79	74.50 ± 9.93	70.78 ± 9.51	84.84 ± 9.11	76.45 ± 8.38
A (cm/s)	49.66 ± 9.15	41.10 ± 9.33	49.79 ± 9.46	43.51 ± 11.47	46.34 ± 9.52
E/A	1.42 ± 0.15	1.87 ± 0.14*	1.46 ± 0.13#	2.05 ± 0.27#	1.81 ± 0.19*
IVCT (ms)	11.14 ± 1.64	12.60 ± 1.67	10.65 ± 1.36#	15.58 ± 0.83#	12.65 ± 2.10
IVRT (ms)	16.12 ± 1.38	17.45 ± 1.73	16.17 ± 1.53	20.01 ± 2.85#	17.67 ± 1.16
DT (ms)	49.93 ± 5.11	46.29 ± 4.37	44.73 ± 4.04	47.35 ± 4.46	45.37 ± 6.27
Tei index	0.55 ± 0.01	0.65 ± 0.02*	0.60 ± 0.01#	0.75 ± 0.04#	0.67 ± 0.02*

All data are expressed as mean ± SD. n represents the number of mice used in each group. *$p < 0.05$ versus sham; #$p < 0.05$ versus +lenti-scramble. TAC, transverse aortic constriction; LV, left ventricular; E, the peak velocities of early rapid filling; A, the peak velocities of late filling; E/A, the ratio of peak velocity of early to late filling of mitral inflow; IVCT, isovolumetric contraction time; IVRT, isovolumic relaxation time; DT, deceleration time of early filling of mitral inflow; Tei index, calculation by the formula (IVRT + IVCT)/ET; +lenti-shUBC9, TAC+lentiviral vector carrying shRNA UBC9; +lenti-shRNF4, TAC+lentiviral vector carrying shRNA RNF4; +lenti-scramble, TAC+lentiviral vector carrying scramble RNA.

(Figure S9), which reduced the levels of TGF-β1 mRNA (Figure 7I) and protein (Figure 7H), suggesting that modulation of the UBC9/PML/RNF4 pathway affects TGF-β1 expression in a Pin1-dependent manner.

DISCUSSION

The results of this study revealed a novel regulatory mechanism of cardiac fibrosis that is composed of UBC9, PML, and RNF4. The present work provides strong evidence that: (1) PML SUMOylation is dynamically changed under varying fibrotic stresses; (2) interference of the dynamic process of PML SUMOylation after silencing UBC9 and RNF4 exerts a potent effect on the maintenance of cardiac structure and function; and (3) the UBC9/PML/RNF4-mediated SUMO pathway regulates the development of cardiac fibrosis, which is associated with Pin1-mediated TGF-β1 expression under various pro-fibrotic stresses.

PML-NBs are profoundly modified in response to different stimuli, including interferon, FBS, CdCl$_2$, heat shock, DNA damage, and inorganic arsenic, the most extensively studied factor. Arsenic has been shown to induce fibrosis in several organs, including the liver,[22] heart,[9] and lungs.[23] In fact, in vitro arsenic treatment can cause a characteristic shift from unmodified PML isoforms to SUMOylated PML in various human and mouse cells.[11,24] Furthermore, one study indicated that PML-NBs accumulate shortly after serum stimulation and promote the translocation of the serum response factor to the NBs in HeLa and NB4 cells.[25] These findings are consistent with the view that multiple pro-fibrotic inducers, including arsenic, Ang II, and FBS, modulate PML SUMOylation and NB distribution in cultured NMCFs.

In the present study, the SUMOylation status and protein expression level of PML were significantly altered by PML overexpression and knockdown. Recent studies by Sun et al.[26] have demonstrated that PML overexpression promotes the osteogenic differentiation of hu-

man mesenchymal stem cells. Similarly, our results showed that PML overexpression induced the differentiation of cardiac fibroblasts into myofibroblasts through the upregulation of α-SMA and TGF-β1 expression. Conversely, our knockdown results (Figure 3) were consistent with those from recent studies showing the impairment of the TGF-β1 signaling pathway in embryonic fibroblasts of PML knockout mice, as evidenced by a reduction in Smad2/3 phosphorylation.[27]

The main emphasis of the present study was on the modification of PML by SUMOs with both in vitro and in vivo experiments. SUMOylation is a critical post-translational modification that can be altered by changes in the level or activity of SUMOylating or de-SUMOylating factors, such as UBC9, SENP, and RNF4. UBC9, a common SUMO conjugation enzyme, targets a multitude of cellular regulators,[5] and numerous groups have demonstrated that ablation of UBC9 expression reduces SUMO conjugation activity.[28,29] Importantly, a recent study showed that UBC9 ablation results in defects in both PML-NB morphogenesis and partner recruitment.[30] Nacerddine et al.[31] observed that loss of UBC9 can lead to defects in PML nuclear architecture and function, contributing to embryonic lethality and mitotic chromosome defects in mammals. Strikingly, one study showed that UBC9 silencing reduced TGF-β receptor type I of the canonical TGF-β signaling pathway, thereby preventing fibrosis.[32] RNF4, a SUMO-dependent ubiquitin E3 ligase that is responsible for the conjugation of ubiquitin with substrate, is recruited following arsenic exposure and triggers SUMO-dependent polyubiquitination of PML. Furthermore, Lallemand-Breitenbach et al. verified that siRNA silencing of RNF4 significantly reduces arsenic-induced degradation of endogenous PML and stabilizes PML SUMOylation in HeLa cells.[12] Additionally, one study found that the loss of PML SUMOylated species after 24 hr exposure to arsenic can be reversed by RNF4 depletion.[24] In support of these studies, our co-IP results (Figure 2C; Figures S2C and S2D) showed a critical link between SUMO-1 or SUMO-2/3 and PML in primary cultured cardiac
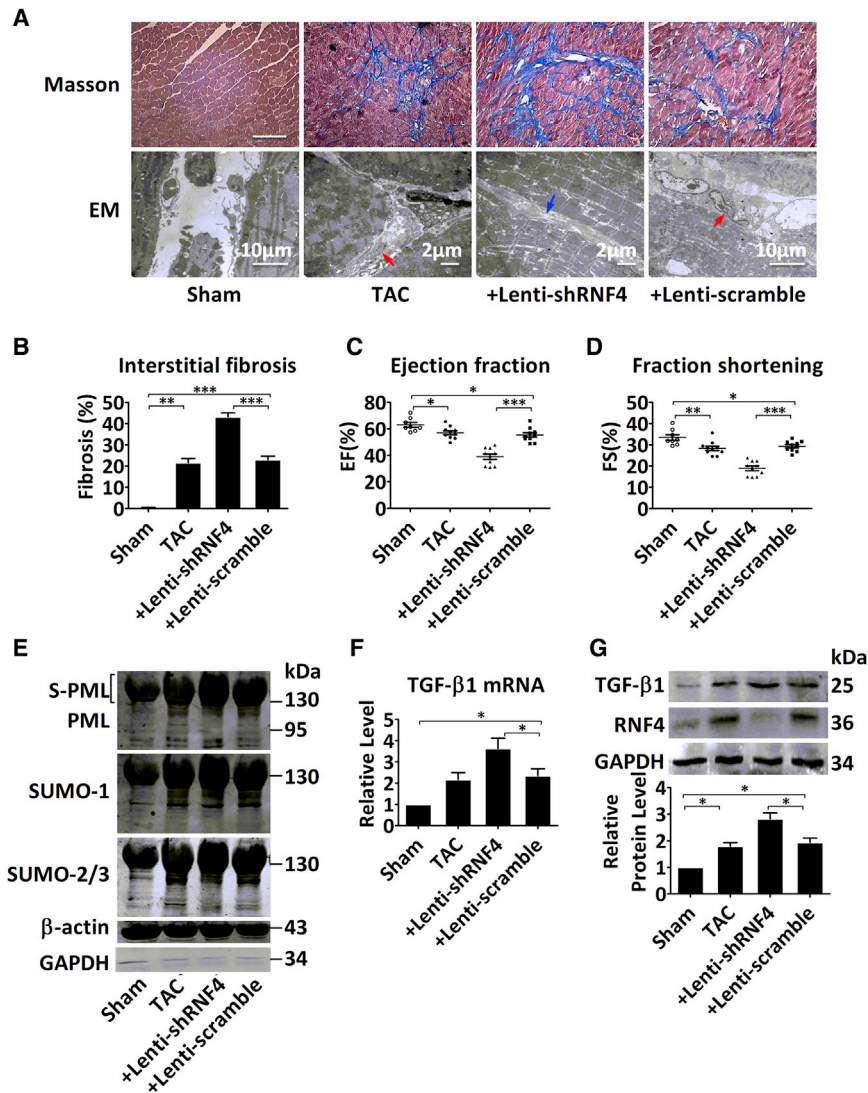
A

Masson

EM

Sham TAC +Lenti-shRNF4 +Lenti-scramble

B Interstitial fibrosis

C Ejection fraction

D Fraction shortening

E

S-PML
PML
SUMO-1
SUMO-2/3
β-actin
GAPDH

kDa
130
95
130
130
43
34

F TGF-β1 mRNA

G

TGF-β1 kDa 25
RNF4 36
GAPDH 34

Figure 6. Knockdown of RNF4 Aggravates Cardiac Fibrosis

(A) Representative images of the left ventricle following Masson's trichrome staining (scale bar, 100 μm) and electron microscopy (EM). The red arrow indicates cardiac fibroblasts, and the blue arrow indicates collagen. (B) Quantification of the fibrotic area (blue) in the indicated histological sections stained with Masson's trichrome. (C and D) The ventricular (C) EF and (D) FS percentages are shown for the four TAC groups at 8 weeks; n = 8–10 per group. (E) Immunoblotting analysis of PML (top), SUMO-1 (middle), and SUMO-2/3 (bottom) in nuclear extracts from mice hearts at 3 weeks after TAC surgery, with β-actin used as a nuclear loading control and GAPDH used as a cytoplasmic loading control. (F and G) Shown here are (F) TGF-β1 mRNA levels analyzed by real-time PCR and (G) TGF-β1 protein levels from the left ventricle of TAC mice at 3 weeks. Data were normalized to GAPDH expression and displayed as mean ± SEM of five independent experiments with similar results. *p < 0.05; **p < 0.01; ***p < 0.001.

extensive interstitial fibrosis. Thus, the global SUMOylation may be a dynamic process in the pathological settings, manifested at the compensated stage, which can cause dynamic modification of PML. As SUMO modifications of PML appear 2–4 weeks post-TAC operation, which is sufficiently long for the activation of the fibrotic signaling, such as TGF-β and Smad, the intervention of PML SUMOylation at the early stages of the pathological process was investigated by knockdown of UBC9 or RNF4.

Interestingly, PML was reported to be degraded in the TAC-induced failing hearts, likely due to SUMO modification that causes degradation following ubiquitin-mediated proteolysis.[7] Thus, the accumulation of SUMOylated PML at early time points may lead to the degradation in the pathological setting. In the present study, the lentivirus-vector constructs were successfully transferred into cardiomyocytes and endothelial cells, in addition to cardiac fibroblasts. As a result, a wide spectrum of cell types, such as cardiomyocytes, inflammatory cells, and endothelial cells, might be under the regulation by PML cooperation with UBC9 and RNF4. If this is true, then UBC9/PML/RNF4 may affect hypertrophic and inflammatory responses, as well as angiogenesis in TAC-induced heart failure. These findings suggest that these key enzymes related to PML activity may contribute to the development of various cardiac diseases.

PML organizes the multi-functional enzymatic structures for many partner proteins, with PML-NBs shown to recruit Pin1 in mammalian cells. Reineke et al.[35] observed that the C-terminal region of PML and the WW-terminal region of Pin1 are required for PML degradation in

fibroblasts. Although knockdown of UBC9 or RNF4 may have effects on global SUMOylation, other SUMO substrates, such as SERCA2a, during heart failure cannot be excluded, and it is possible that UBC9 or RNF4 depletion could partially alter SUMO conjugation onto PML in the established pathological setting.

Overall, PML SUMOylation was significantly increased at the early compensatory stage (at 2 weeks post-TAC) during the transition to heart failure, which was in accordance with the observations by Ahyoung Lee et al.[33,34] that the supply of SUMO-1 is increased slightly during the compensated stage of hypertrophy, followed by a sharp decrease in mice undergoing TAC. Moreover, Eun Young Kim et al.[34] have demonstrated that the severity of cardiac phenotypes is closely associated with SUMO-2 conjugation levels in the heart, as indicated by SUMO overexpression in transgenic mice that exhibit cardiac dysfunction in the setting of cardiac hypertrophy with
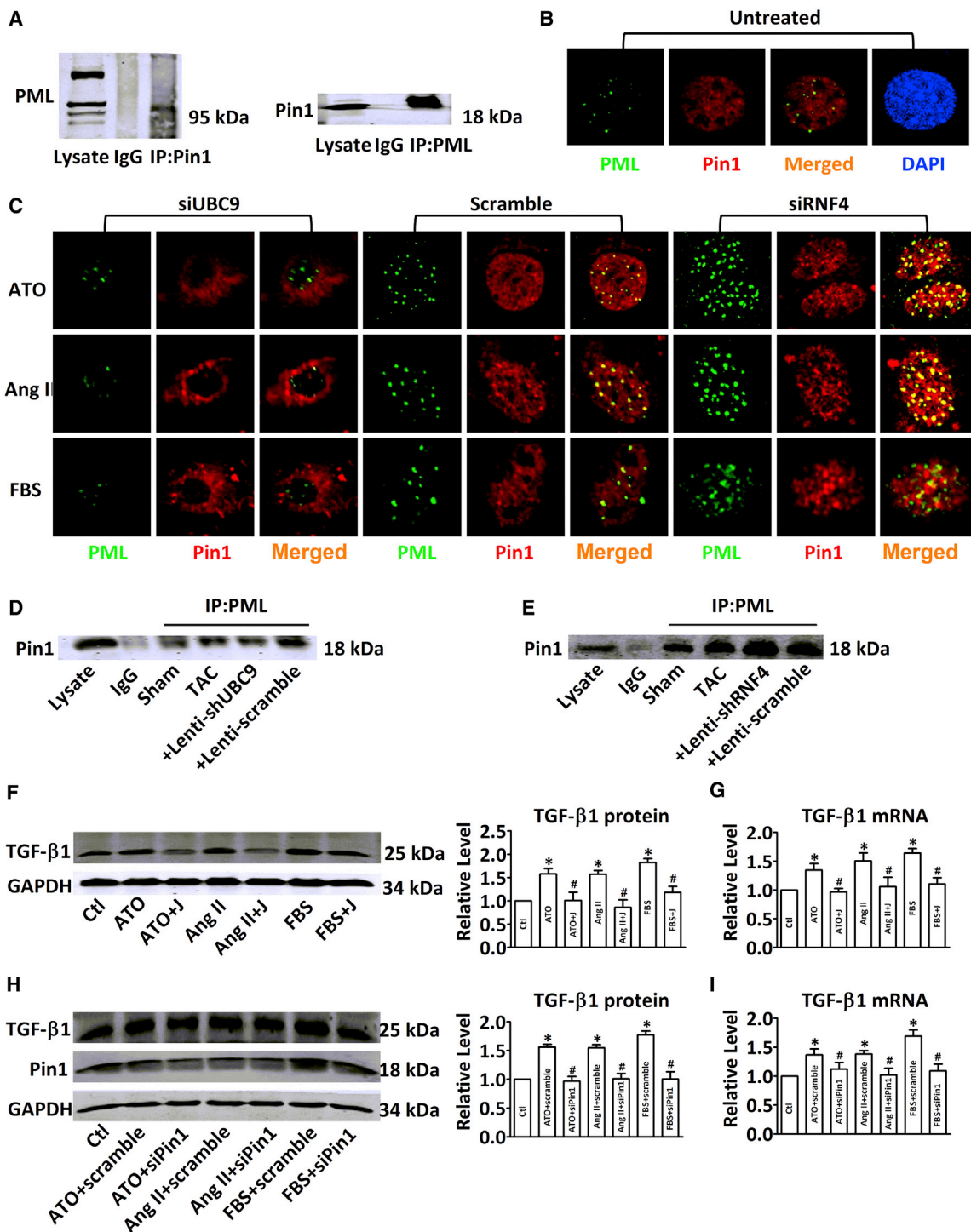
Figure 7. Silencing of UBC9 and RNF4 Modulates the Interaction between PML and Pin1

(A) Interaction of PML with Pin1 in heart tissue was analyzed by co-IP. Total heart lysates from KM mice immunoprecipitated with either anti-Pin1 or anti-PML antibody were able to be pulled down with either PML (95 kDa) or Pin1. IgG, immunoglobulin G. (B) Representative immunofluorescent staining of NMCFs immunostained with specific antibodies against PML (green), Pin1 (red), and DAPI (blue) to label nuclei. The amplified view of the cells provided in Figure S6. (C) Representative immunofluorescent image showing endogenous co-localization of PML (green) and Pin1 (red) after transfection with siRNA specific for UBC9 or RNF4 and treatment with 2 μM ATO for 4 hr and 100 nM Ang II or 20% FBS for 12 hr. (D and E) The nuclear lysates were immunoprecipitated with anti-PML antibodies, and immunoblotting was performed with a Pin1 antibody after

(legend continued on next page)

a phosphorylation-dependent manner. Another study by Asmi et al.[36] demonstrated that PML IV induces recruitment of Pin1 into PML-NBs and positively regulates IRF3-dependent synthesis of interferon in response to viral infections. Additionally, several studies have suggested that Pin1 and TGF-β1 production are related to the development of fibrosis. Shen et al.[18] showed that Pin1 increases TGF-β1 expression by regulating the association of several ARE-binding proteins in human and murine eosinophils, leading to allergic lung fibrosis. Moreover, one study reported that TGF-β1 expression and TGF-β1-mediated fibrosis in human and mouse fibrotic livers occur in a Pin1-dependent manner and are involved in PI3K (phosphatidylinositol 3-kinase)/Akt- or ERK-mediated activator protein-1 (AP-1) phosphorylation.[37] Previous studies have linked Pin1 to the TGF-β1-dependent Smad2/3 activation in lung and liver fibrosis. Regardless of its pleiotropic effect in fibrosis, TGF-β1, and its related signaling elements, also regulates the adaptive growth of cardiomyocytes in response to hypertrophic stress.[38] Furthermore, Pin1 was also found to serve as a novel modulator regulating cardiac hypertrophy, with its expression increased in the hearts of TAC-pressure overload mice.[39] These reports are consistent with the present study, indicating that increased TGF-β1 expression is associated with Pin1 sequestration into PML bodies and may exert pro-hypertrophic functions.

The association of the SUMO conjugation with cardiac disease is a new discovery, and the importance of the SUMO pathway in the development and maintenance of the normal cardiovascular system is just emerging. Herein, for the first time, we identified the SUMO-dependent pathway—composed of UBC9, PML, and RNF4—as a critical determinant for the development of myocardial fibrosis.

MATERIALS AND METHODS
The methods used in this study are provided in detail in the Supplemental Information.

Animals
All animal experiments were performed in accordance with the NIH guidelines (Guide for the Care and Use of Laboratory Animals) and approved by the Institutional Animal Care and Use Committee of Harbin Medical University, P.R. China. Kunming (KM) mice used in this study were provided by the Experimental Animal Center of Harbin Medical University (Grade II). KM mice were anesthetized with sodium pentobarbitone (40 mg/kg, intraperitoneally [i.p.]) and xylazine (12.5 mg/kg, i.p.). The absence of withdrawal reflex to tail pinch was used to assess the adequacy of anesthesia. Detailed methods for establishing the experimental fibrotic models are described in the Supplemental Information. After surgery, mice were euthanized by cervical dislocation following CO_2 inhalation.

Lentivirus Infection In Vivo
After anesthetization, the LV cavity of KM mice was injected with lentivirus that carries shRNA or scramble shRNA (2.5×10^7 TUs [transfection units]/mL in 100 μL) (Invitrogen) through the tip of the heart using a 30G syringe. Artery occlusion remained for 10 s following lentivirus injection.

Echocardiographic Measurement
Echocardiography was performed using an ultrasound machine (Vivid 7 GE Medical) with a 10-MHz phase-array transducer. Viable mice after TAC were subjected to echocardiography to assess the left ventricular function. Two-dimensional and M-mode images were obtained in the short-axis view to assess the systolic function.

Pulse Wave Doppler
The apical four-chamber view or LV long-axis view was used for transmitral inflow Doppler to evaluate the LV diastolic function in mice. The Doppler indices included the ratio of peak velocity of early to late filling of mitral inflow (E/A ratio), deceleration time (DT) of early filling of mitral inflow, isovolumetric relaxation time (IVRT), and isovolumetric contraction time (IVCT). The E/A ratio and the Tei index were calculated using the formula (IVRT + IVCT)/ET for the assessment of the diastolic function.

Masson Staining
Heart samples were immersed in 4% paraformaldehyde and embedded in paraffin. After 24 hr, samples were stained with Masson's trichrome (Accustain HT15, Sigma-Aldrich) to assess the extent of interstitial fibrosis. Tissues were imaged at 200× by bright-field microscopy (IX71 Olympus). The quantity of cardiac fibrosis was determined by the ratio of collagen surface area to total myocardial surface area. Image analysis software (Image-Pro Plus v4.0; Meida Cybernetics) was used to evaluate collagen deposition.

Transmission Electron Microscopy
Hearts were fixed in 2.5% glutaraldehyde (pH 7.4) overnight and dehydrated with a series of ethanol gradients. Samples were embedded in Epon and cut into ultrathin sections (60–70 nm). After staining with uranyl acetate and lead citrate, sections of the left ventricle were observed under a JEOL 1200 electron microscope (JEOL).

Cardiac Fibroblast Culture and siRNA Transfection
NMCFs were obtained from 1- to 3-day-old KM mice. The animals were anesthetized by 4% isoflurane inhalation before rapid heart excision, and adequate anesthesia was monitored by the absence of reflexes. Detailed information about cell culture and transfection are provided in the Supplemental Information.

---

shRNA transfection targeting (D) UBC9 or (E) RNF4. (F and G) As shown here, (F) TGF-β1 protein levels were measured by immunoblotting, and (G) mRNA levels were determined by real-time PCR following treatment with ATO (2 μM) for 4 hr and Ang II (100 nM) or FBS (20%) for 12 hr after the addition of Juglone (5 μM) for 4 hr. (H and I) As shown here, (H) TGF-β1 protein levels were determined by immunoblotting analysis, and (I) mRNA levels were quantified by real-time PCR following treatment with ATO (2 μM) for 4 hr and Ang II (100 nM) or FBS (20%) for 12 hr after transfection of siRNA against Pin1 for 6 hr. Data shown in (A)–(E) are representative of three independent experiments with similar results. Data were normalized to GAPDH expressed as mean ± SEM. *p < 0.05 versus control; #p < 0.05 versus ATO-, AngII-, or FBS-treated groups. See also Figure S6.

Measurement of Collagen Content

Total collagen content in NMCFs was determined using the Sircol Collagen Assay Kit (Biocolor) following the manufacturer's protocol.

Immunoblotting

Total protein was extracted from whole cells and tissues as described in the Supplemental Experimental Procedures. The nuclear protein was obtained according to the manufacturer's protocol (NE-PER Kit, Pierce Biotechnology). Protein samples were separated on 10% or 12% SDS-PAGE gels and transferred to nitrocellulose filter membranes, which were then probed with specific primary antibodies.

Real-Time qPCR

Total RNA was extracted and analyzed according to the manufacturer's protocols (TRIzol, Invitrogen). Detailed information is included in the Supplemental Information.

Co-IP

Lysates were incubated with specific antibodies and then conjugated with protein A/G agarose beads. After centrifugation, the beads were collected and rinsed gently. The samples were denatured and then analyzed using SDS-PAGE to detect the interaction between two protein partners.

Immunofluorescence Staining

After permeabilization and blocking, the cells were incubated with specific antibodies, and the fluorescence was detected with a laser-scanning confocal microscope (Olympus).

Statistical Analysis

Statistical analysis was performed with GraphPad Prism (Graphpad Software). Comparisons between two groups were determined by Student's t test. Multiple-group comparisons were performed by one-way ANOVA followed by the Tukey procedure for comparison of mean values. A value of $p < 0.05$ was considered to be statistically significant.

SUPPLEMENTAL INFORMATION

Supplemental Information includes Supporting Materials and Methods, nine figures, and two tables and can be found with this article online at http://dx.doi.org/10.1016/j.ymthe.2016.12.021.

AUTHOR CONTRIBUTIONS

B.-F.Y. and W.-F.C. conceived and designed the experiments. Y.L. and D.Z. contributed to the manuscript writing. F.Q. analyzed the data. L.-L.Z., S.-K.L., and Y.-Y.L. performed animal models. M.-T.L., D.W., and J.-X.W. conducted the in vitro experiments. X.-Q.D. and Y.-X.L. were responsible for cell culture. The echocardiography was performed by C.-J.D. and X.-Q.S.

CONFLICTS OF INTEREST

The authors declare no competing financial interests.

REFERENCES

1. Kho, C., Lee, A., Jeong, D., Oh, J.G., Gorski, P.A., Fish, K., Sanchez, R., DeVita, R.J., Christensen, G., Dahl, R., and Hajjar, R.J. (2015). Small-molecule activation of SERCA2a SUMOylation for the treatment of heart failure. Nat. Commun. 6, 7229.

2. Weber, K.T., and Brilla, C.G. (1991). Pathological hypertrophy and cardiac interstitium. Fibrosis and renin-angiotensin-aldosterone system. Circulation 83, 1849–1865.

3. Derynck, R., and Zhang, Y.E. (2003). Smad-dependent and Smad-independent pathways in TGF-beta family signalling. Nature 425, 577–584.

4. Bujak, M., and Frangogiannis, N.G. (2007). The role of TGF-beta signaling in myocardial infarction and cardiac remodeling. Cardiovasc. Res. 74, 184–195.

5. Hay, R.T. (2005). SUMO: a history of modification. Mol. Cell 18, 1–12.

6. Zhang, X.W., Yan, X.J., Zhou, Z.R., Yang, F.F., Wu, Z.Y., Sun, H.B., Liang, W.X., Song, A.X., Lallemand-Breitenbach, V., Jeanne, M., et al. (2010). Arsenic trioxide controls the fate of the PML-RARalpha oncoprotein by directly binding PML. Science 328, 240–243.

7. Tatham, M.H., Geoffroy, M.C., Shen, L., Plechanovova, A., Hattersley, N., Jaffray, E.G., Palvimo, J.J., and Hay, R.T. (2008). RNF4 is a poly-SUMO-specific E3 ubiquitin ligase required for arsenic-induced PML degradation. Nat. Cell Biol. 10, 538–546.

8. Lallemand-Breitenbach, V., and de Thé, H. (2010). PML nuclear bodies. Cold Spring Harb. Perspect. Biol. 2, a000661.

9. Chu, W., Li, C., Qu, X., Zhao, D., Wang, X., Yu, X., Cai, F., Liang, H., Zhang, Y., Zhao, X., et al. (2012). Arsenic-induced interstitial myocardial fibrosis reveals a new insight into drug-induced long QT syndrome. Cardiovasc. Res. 96, 90–98.

10. Regad, T., and Chelbi-Alix, M.K. (2001). Role and fate of PML nuclear bodies in response to interferon and viral infections. Oncogene 20, 7274–7286.

11. Lallemand-Breitenbach, V., Zhu, J., Puvion, F., Koken, M., Honoré, N., Doubeikovsky, A., Duprez, E., Pandolfi, P.P., Puvion, E., Freemont, P., and de Thé, H. (2001). Role of promyelocytic leukemia (PML) sumolation in nuclear body formation, 11S proteasome recruitment, and As2O3-induced PML or PML/retinoic acid receptor alpha degradation. J. Exp. Med. 193, 1361–1371.

12. Lallemand-Breitenbach, V., Jeanne, M., Benhenda, S., Nasr, R., Lei, M., Peres, L., Zhou, J., Zhu, J., Raught, B., and de Thé, H. (2008). Arsenic degrades PML or PML-RARalpha through a SUMO-triggered RNF4/ubiquitin-mediated pathway. Nat. Cell Biol. 10, 547–555.

13. Shen, T.H., Lin, H.K., Scaglioni, P.P., Yung, T.M., and Pandolfi, P.P. (2006). The mechanisms of PML-nuclear body formation. Mol. Cell 24, 331–339.

14. Tatham, M.H., Jaffray, E., Vaughan, O.A., Desterro, J.M., Botting, C.H., Naismith, J.H., and Hay, R.T. (2001). Polymeric chains of SUMO-2 and SUMO-3 are conjugated to protein substrates by SAE1/SAE2 and Ubc9. J. Biol. Chem. 276, 35368–35374.

15. Sun, H., Leverson, J.D., and Hunter, T. (2007). Conserved function of RNF4 family proteins in eukaryotes: targeting a ubiquitin ligase to SUMOylated proteins. EMBO J. 26, 4102–4112.

16. Kawaguchi, M., Hay, I., Fetics, B., and Kass, D.A. (2003). Combined ventricular systolic and arterial stiffening in patients with heart failure and preserved ejection fraction: implications for systolic and diastolic reserve limitations. Circulation 107, 714–720.

17. Burlew, B.S., and Weber, K.T. (2002). Cardiac fibrosis as a cause of diastolic dysfunction. Herz 27, 92–98.

18. Shen, Z.J., Esnault, S., Rosenthal, L.A., Szakaly, R.J., Sorkness, R.L., Westmark, P.R., Sandor, M., and Malter, J.S. (2008). Pin1 regulates TGF-beta1 production by activated

human and murine eosinophils and contributes to allergic lung fibrosis. J. Clin. Invest. *118*, 479–490.

19. Wu, J., Zhou, L.Q., Yu, W., Zhao, Z.G., Xie, X.M., Wang, W.T., Xiong, J., Li, M., Xue, Z., Wang, X., et al. (2014). PML4 facilitates erythroid differentiation by enhancing the transcriptional activity of GATA-1. Blood *123*, 261–270.

20. Kuo, H.Y., Chen, Y.C., Chang, H.Y., Jeng, J.C., Lin, E.H., Pan, C.M., Chang, Y.W., Wang, M.L., Chou, Y.T., Shih, H.M., and Wu, C.W. (2013). The PML isoform IV is a negative regulator of nuclear EGFR's transcriptional activity in lung cancer. Carcinogenesis *34*, 1708–1716.

21. Chao, S.H., Greenleaf, A.L., and Price, D.H. (2001). Juglone, an inhibitor of the peptidyl-prolyl isomerase Pin1, also directly blocks transcription. Nucleic Acids Res. *29*, 767–773.

22. Wu, J., Liu, J., Waalkes, M.P., Cheng, M.L., Li, L., Li, C.X., and Yang, Q. (2008). High dietary fat exacerbates arsenic-induced liver fibrosis in mice. Exp. Biol. Med. (Maywood) *233*, 377–384.

23. Heck, J.E., Andrew, A.S., Onega, T., Rigas, J.R., Jackson, B.P., Karagas, M.R., and Duell, E.J. (2009). Lung cancer in a U.S. population with low to moderate arsenic exposure. Environ. Health Perspect. *117*, 1718–1723.

24. Sahin, U., Ferhi, O., Jeanne, M., Benhenda, S., Berthier, C., Jollivet, F., Niwa-Kawakita, M., Faklaris, O., Setterblad, N., de Thé, H., and Lallemand-Breitenbach, V. (2014). Oxidative stress-induced assembly of PML nuclear bodies controls sumoylation of partner proteins. J. Cell Biol. *204*, 931–945.

25. Matsuzaki, K., Minami, T., Tojo, M., Honda, Y., Saitoh, N., Nagahiro, S., Saya, H., and Nakao, M. (2003). PML-nuclear bodies are involved in cellular serum response. Genes Cells *8*, 275–286.

26. Sun, J., Fu, S., Zhong, W., and Huang, H. (2013). PML overexpression inhibits proliferation and promotes the osteogenic differentiation of human mesenchymal stem cells. Oncol. Rep. *30*, 2785–2794.

27. Tang, M.K., Liang, Y.J., Chan, J.Y., Wong, S.W., Chen, E., Yao, Y., Gan, J., Xiao, L., Leung, H.C., Kung, H.F., et al. (2013). Promyelocytic leukemia (PML) protein plays important roles in regulating cell adhesion, morphology, proliferation and migration. PLoS ONE *8*, e59477.

28. He, X., Riceberg, J., Pulukuri, S.M., Grossman, S., Shinde, V., Shah, P., Brownell, J.E., Dick, L., Newcomb, J., and Bence, N. (2015). Characterization of the loss of SUMO pathway function on cancer cells and tumor proliferation. PLoS ONE *10*, e0123882.

29. Sahin, U., Lapaquette, P., Andrieux, A., Faure, G., and Dejean, A. (2014). Sumoylation of human argonaute 2 at lysine-402 regulates its stability. PLoS ONE *9*, e102957.

30. Rojas-Fernandez, A., Plechanovová, A., Hattersley, N., Jaffray, E., Tatham, M.H., and Hay, R.T. (2014). SUMO chain-induced dimerization activates RNF4. Mol. Cell *53*, 880–892.

31. Nacerddine, K., Lehembre, F., Bhaumik, M., Artus, J., Cohen-Tannoudji, M., Babinet, C., Pandolfi, P.P., and Dejean, A. (2005). The SUMO pathway is essential for nuclear integrity and chromosome segregation in mice. Dev. Cell *9*, 769–779.

32. Khodzhigorova, A., Distler, A., Lang, V., Dees, C., Schneider, H., Beyer, C., Gelse, K., Distler, O., Schett, G., and Distler, J.H. (2012). Inhibition of sumoylation prevents experimental fibrosis. Ann. Rheum. Dis. *71*, 1904–1908.

33. Lee, A., Jeong, D., Mitsuyama, S., Oh, J.G., Liang, L., Ikeda, Y., Sadoshima, J., Hajjar, R.J., and Kho, C. (2014). The role of SUMO-1 in cardiac oxidative stress and hypertrophy. Antioxid. Redox Signal. *21*, 1986–2001.

34. Kim, E.Y., Zhang, Y., Beketaev, I., Segura, A.M., Yu, W., Xi, Y., Chang, J., and Wang, J. (2015). SENP5, a SUMO isopeptidase, induces apoptosis and cardiomyopathy. J. Mol. Cell. Cardiol. *78*, 154–164.

35. Reineke, E.L., Lam, M., Liu, Q., Liu, Y., Stanya, K.J., Chang, K.S., Means, A.R., and Kao, H.Y. (2008). Degradation of the tumor suppressor PML by Pin1 contributes to the cancer phenotype of breast cancer MDA-MB-231 cells. Mol. Cell. Biol. *28*, 997–1006.

36. El Asmi, F., Maroui, M.A., Dutrieux, J., Blondel, D., Nisole, S., and Chelbi-Alix, M.K. (2014). Implication of PMLIV in both intrinsic and innate immunity. PLoS Pathog. *10*, e1003975.

37. Shen, Z.J., Braun, R.K., Hu, J., Xie, Q., Chu, H., Love, R.B., Stodola, L.A., Rosenthal, L.A., Szakaly, R.J., Sorkness, R.L., and Malter, J.S. (2012). Pin1 protein regulates Smad protein signaling and pulmonary fibrosis. J. Biol. Chem. *287*, 23294–23305.

38. Wang, J., Xu, N., Feng, X., Hou, N., Zhang, J., Cheng, X., Chen, Y., Zhang, Y., and Yang, X. (2005). Targeted disruption of Smad4 in cardiomyocytes results in cardiac hypertrophy and heart failure. Circ. Res. *97*, 821–828.

39. Toko, H., Konstandin, M.H., Doroudgar, S., Ormachea, L., Joyo, E., Joyo, A.Y., Din, S., Gude, N.A., Collins, B., Völkers, M., et al. (2013). Regulation of cardiac hypertrophic signaling by prolyl isomerase Pin1. Circ. Res. *112*, 1244–1252.